Phys Chem Minerals (1999) 26: 513–520

ORIGINAL PAPER

N.S. Bagdassarov

Viscoelastic behaviour of mica-based glass-ceramic aggregate

Received: 26 June 1998 / Revised, accepted: 13 January 1999

Abstract The present study deals with the small strain torsion deformation of MACOR glass-ceramic samples at high temperatures (450–850 °C) and over a range of low frequencies (20 Hz–5 mHz). The samples of MACOR ceramic consist of 55 vol% randomly oriented, sheet-like fluorophlogopite mica crystals (~100–20 μm in planar size, 1–2 μm in thickness) and 45 vol% of isotropic alumino-borosilicate glass matrix. Measurements of the complex shear modulus show that the sample does not possess the relaxed shear viscosity even at temperatures above the glass transition temperature of the glass matrix. The maximum of the imaginary component $G''(\omega)$ of the shear modulus is ~0.15 of the unrelaxed value G_∞, the relaxation strength $\Delta \approx 0.9$. The activation energy of the peak of $G''(\omega)$ is ~245 kJ mol^{-1}. Using this value of E_a, the data obtained at various frequencies and temperatures have been reduced to a master curve using the dimensionless variable $\omega\tau$, where $\tau \sim \tau_0 \exp(-E_a/RT)$. The internal friction $Q^{-1}(\omega\tau)$ is $\propto 1/(\omega\tau)^{0.35-0.4}$ in the low-temperature high-frequency range ($\omega\tau \gg 1$); passes through a maximum at $\omega\tau \sim 1$ and trends asymptotically to a value $Q^{-1} \sim 0.25$–0.30 at $\omega\tau \ll 1$. The behaviour of $Q^{-1}(\omega\tau)$ differs from that of a Caputo body by the presence of the resolved peak which may be attributed to the slow mechanical relaxation of mica crystals due to rotation as well as flexing and bending modes of crystal deformation.

Key words MACOR glass-ceramic · Shear stress relaxation · Anelasticity · Viscoelasticity · Complex shear modulus · Internal friction

N.S. Bagdassarov
Institut für Meteorologie und Geophysik,
Universität Frankfurt, Feldbergstraße 47,
D-60323 Frankfurt, Germany
e-mail: nickbagd@geophysik.uni-frankfurt.de

Introduction

Knowledge of the characteristics of viscoelastic and anelastic behaviour of mica-based glass-ceramic materials such as internal friction, complex shear modulus and viscosity are essential to understanding their toughness, anelasticity and workability. In addition these studies may be useful to compare the complex rheology of essentially 2-D crystal-melt aggregates, in which crystals have a high aspect ratio, with 3-D crystal-melt aggregates (e.g. Raj and Chyung 1981). Fluormica glass-ceramics represent an almost 2-D crystal-melt aggregate. During deformation of this material mica crystals can be easily delaminated due to their low cleavage energy in directions parallel to the flat crystals. This results in machinability, i.e. the ease with which these ceramics are cut (Baik et al. 1995). Machinability of this material with conventional tools ensures its wide industrial use as an engineering ceramic or dental inlay (Beall et al. 1974, 1978).

Usually, anelastic behaviour, i.e. the internal friction spectroscopy Q^{-1} as function of frequency and temperature, of crystal-melt aggregates is studied by using a torsion oscillation pendulum (e.g. Kê 1949; Day and Rindone 1961; Weiner et al. 1987; Versteeg and Kohlstedt 1994). These studies have revealed a well-defined high temperature peak associated with crystal grain boundary sliding. For example, this peak appears at the volume fraction of the lithium disilicate >55 vol% in the $Li_2O{*}2.75SiO_2$ system (Day and Rindone 1961). The amplitude of the peak increases and the shape is considerably broadened with the increase of the volume content of crystals. At the same time any low temperature peaks vanished. Internal friction in LAS glass-ceramics with several vol% of glass (>95 vol. % of β-spodumene grains, size 0.9–2 μm) was studied up to 1100 °C (Versteeg and Kohlstedt 1994). The amplitude of the high temperature peak in the crystal-melt aggregate with several percent of liquid phase is associated with grain boundary sliding and correlated with the grain boundary chemistry (glass composition).

The present experimental study aimed to estimate the internal friction of the glass-ceramic aggregate which had mica-crystals with this large aspect ratio, and, thus, to complement the previous viscoelastic study of crystal-melt suspensions (Bagdassarov et al. 1994).

Experiments

Sample description

The sample used in experiments is MACOR an isotropic glass-ceramic, product of Corning Glass, Inc. The MACOR glass-ceramic is a fluorine-rich glass with a starting composition close to that of trisilicic fluorophlogopite mica ($KMg_3AlSi_3O_{10}F_2$). The composition of the matrix glass is SiO_2 - 35–45 wt.%, Al_2O_3 - 14–19, MgO - 16–24, K_2O - 4–6, $B_2O_3 \sim 5$–10, F^- - 6–10 (Beall et al. 1974). Annealing and devitrification of the starting glass composition results in a series of morphological changes and formation of randomly oriented, sheet-like fluorophlogopite mica crystals in the alumino-borosilicate matrix (Beall et al. 1974, 1978). The crystal structure represents a "house-of-cards" framework in the isotropic glass matrix (Fig. 1). The fluormica crystals are highly interlocked in a glass matrix. The indentation deformation takes the form of local shear microfractures along the mica-glass interfaces (Lawn et al. 1994). The macroscopical manifestation of this deformation in an effective "ductility" of the material, which permits continuous cutting of this glass-ceramic without microscopic fracture. The average dimensions of crystals measured on a SEM are 100–20 μm in both *a* and *b* crystallographic directions and about 1–2 μm in *c* direction. The volume fraction of crystals is about 52–56 vol%, estimated by image analysis of SEM pictures. The growth of this shape of crystal with such high aspect ratios is a result of (1) starving the original glass of K_2O, i.e. the depletion of alkalis for the interlayer cation of growing crystals, and (2) the addition of B_2O_3 to the original glass, which serves to lower the viscosity of the original 'green' glass and thus allows rapid growth in the *a* and *b* directions of fluormica crystals (Beall 1972).

The density of the MACOR samples, determined by Archimedean buoyancy determinations (in toluene and air) using a laboratory Mettler AE 160 balance (precision 10^{-4} g) is 2.543 ± 0.004 g cm^{-3}. The unrelaxed shear modulus has been measured at 20 °C on an ANUTECH ultrasonic interferometer described elsewhere (Jackson et al. 1981) is $G_\infty = 25.55 \pm 0.05$ GPa. The thermal expansion coefficient has been measured in this study by vertical push-rod dilatometry (Model TMA 402, Netzsch Gerätebau, Selb, Germany), using a heating rate of 5 K min^{-1}. Between temperatures 50–450 °C the volume thermal expansion coefficient α_T is almost a constant $27 \pm 1 \times 10^{-6}$°C^{-1} (the linear thermal expansion coefficient is 9×10^{-6} °C^{-1}). From temperatures 470–525 °C α_T linearly increases to a maximum value $60 \pm 1 \times 10^{-6}$ °C^{-1} (the linear thermal expansion rate increases to 20×10^{-6} °C^{-1}). The temperature interval 515–525 °C, can be considered as a softening temperature (softening of a glassy phase in the aggregate). With the further temperature increase α_T oscillates around 50×10^{-6} °C^{-1} reaching a minimum value of 30×10^{-6} °C^{-1} at 850 °C. Above 850 °C α_T increases again reaching a value of 65×10^{-6} °C^{-1} at 930 °C. Comparison of SEM images of the sample thin sections before and after annealing at 930 °C over 2 h did not reveal any significant morphological changes in MACOR glass-ceramic samples (Fig. 1). The measured thermal expansion coefficient has been used for the thermal correction of sample dimensions of the complex shear modulus calculations.

Fig. 1 SEM photo of MACOR sample annealed for 2 h at 930 °C

Torsion deformation study

The cylindrical samples (diameter 8 mm, length 20 mm) have been machined from a cylindrical bar of MACOR ceramic and the flat ends of cylinders were machined to conical surfaces (angle ≈2°). The prepared MACOR glass-ceramic samples were placed between two alumina rods (Al23-Frialit-Degussit, diameter 8 mm, length ≈190 mm) used as holders in the oscillatory torsion deformation apparatus. The inverse conical surfaces (the same angle and depth as for samples) were machined on the flat ends of alumina rods. The conical grips of sample have been glued into the conical holes of alumina rods with a high temperature cement Polytec and annealed at 500 °C for 6 h. During annealing a small axial force of about 8 N from a flat spring was applied to the aligned assemblage of two alumina rods and a sample between them. The mechanical contact between the alumina rods and MACOR sample was tested at 20–450 °C by measuring the phase delay between applied sinusoidal torque and resulted twist deformation at two points on the alumina rods. The axial load 3–5 N was exerted on the assemblage of two rods and a sample during experiments. When a small strain torsion deformation was applied (maximum 2×10^{-2} N m), no slipping in mechanical contact was observed within the precision of the twist deformation measurement (maximum 2×10^{-4} rad). A detailed description of the oscillatory torsion deformation device, its operational principle and the calibration procedure has been described elsewhere (Bagdassarov and Dingwell 1993). This device has been already used for measurements of the internal friction in partially molten rocks (Berckhemer et al. 1982; Bagdassarov and Dorfman 1998) and for the complex shear modulus and viscosity measurements in silicate melts at high temperatures (Bagdassarov and Dingwell 1993; Bagdassarov et al. 1993).

Analysis of data

The measurements of complex shear modulus and phase delay between applied torque and resulted twist deformation were made in the frequency range $f = 20$ Hz–5 mHz and at temperatures of 450–850 °C. The results of complex shear modulus and loss angle (or phase delay between applied torque and the resulting angular deformation of the sample), are shown in Figs. 2 and 3 as a function of angular velocity $\omega = 2\pi f$. Below a temperature of 450 °C the shear modulus of the ceramic sample does not depend on the frequency, within the experimental error. At high temperatures above the softening temperature range of the interstitial glass and at low frequencies, the shear modulus is also constant ≈1.9–2.0 GPa as well as the internal friction ≈0.2. Thus, the concentration of disk-shape crystals is enough to support applied shear stresses and the aggregate possesses a "skeleton structure" which is revealed via a non-zero relaxed shear modulus. The phase delay as a function of frequency has a maximum value. The frequency of

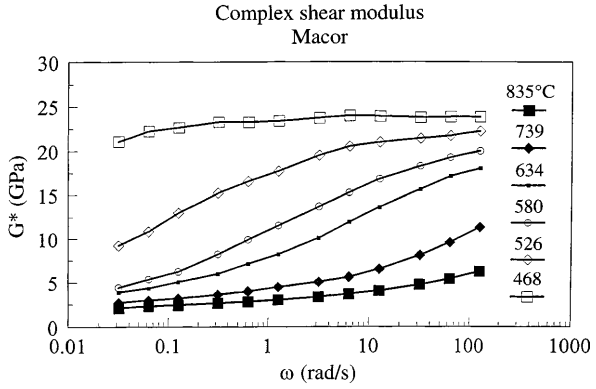

Fig. 2 Complex shear modulus of MACOR sample as function of angular velocity ω

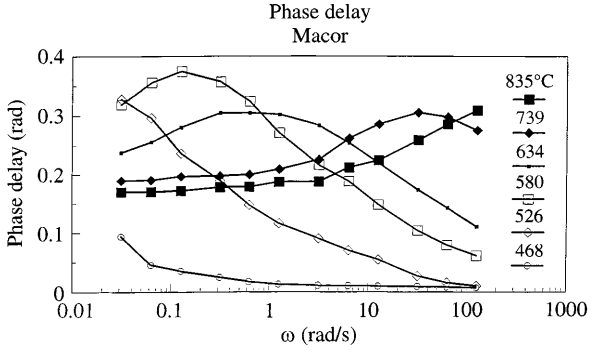

Fig. 3 Phase delay in the MACOR sample as a function of angular velocity ω

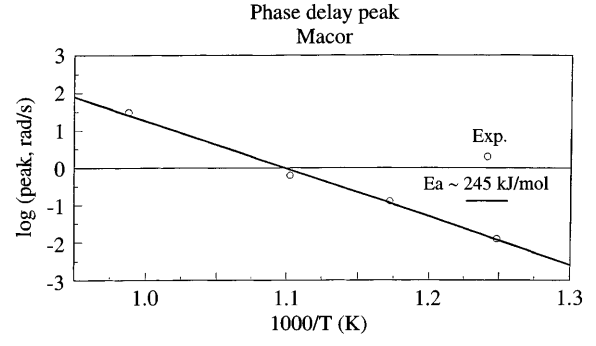

Fig. 4 Arrhenius dependence of the phase delay peak of MACOR sample

deformation corresponding to a maximum of phase delay in the sample decreases with temperature increase. Figure 4 shows this tendency. The slope of the Arrhenius plot $ln(\omega_{peak}) \propto 1/T,K$ has an activation energy of 245 kJ mol^{-1} close to the activation energy of viscous flow for alumino-borosilicate melts (Dingwell et al. 1992). This value E_a has been used to reduce the data obtained at different temperatures and frequencies on a master curve as a function of the dimensionless variable ωτ, where τ is a relaxation time:

$$\tau = \tau_o \exp\left(-\frac{Ea}{RT}\right) \tag{1}$$

where parameter τ_o was chosen to fit the condition that the maximum of $Q^{-1}(\omega\tau)$ corresponds to $\omega\tau \approx 1$. The master curves of the internal friction $Q^{-1}(\omega\tau)$ and of the normalised component of shear modulus $Re[G(\omega\tau)/G_\infty]$, $Im[G(\omega\tau)/G_\infty]$ are shown in Figs. 5 and 6, respectively. The master curve of the complex shear modulus shows that the normalised maximum of the imaginary component of shear modulus *max*. G' is $0.15–0.17G_\infty$, which is much less than that for a Maxwell body (*max*. $G'' = 0.5G_\infty$) and likely corresponds to a Caputo body

$$G'_{\max} = 0.5G_\infty \frac{\sin\left(\frac{\gamma\pi}{2}\right)}{1+\cos\left(\frac{\gamma\pi}{2}\right)} \tag{2}$$

with $\gamma \approx 0.4$ (Caputo 1967). The shape of the peak of the imaginary component of the shear modulus is symmetrical, with the extended left and right shoulders for more than 4 log units of ωτ at the level of *max*. $G''/2$, indicating a significant deviation from a Maxwell liquid (single relaxation time) behaviour even at low frequency–high temperature states. The real component of the shear modulus has a non-zero plateau at $\omega\tau \to 0$. The internal friction has a maximum (Fig. 5) and asymptotically tends towards the value of 0.15–0.2 at the low frequency–high temperature range. At $\omega\tau \gg 1$ (high frequency-low temperature range) the internal friction $Q^{-1}(\omega\tau) \propto 1/(\omega\tau)^{0.3-0.4}$. The Cole–Cole diagram, which is shown in Fig. 7, also deviates from the shape of the Cole–Cole diagrams of the known viscoelastic bodies by having a non-zero real component of shear modulus ($\approx 0.1\ G_\infty$) at a negligible small imaginary component G''. The width of the $Q^{-1}(\omega\tau)$ peak at half of maximum is approximately 2.0–2.2 log units of ω. This means that the distribution parameter β* in the lognormal relaxation spectrum is about 2.5 (Tsai and Raj 1980). The observed relaxation strength of the shear modulus $\Delta = (G_\infty - G_o)/G_\infty = 0.9$. If the relaxation spectrum corresponds to a lognormal distribution, this relaxation strength and β* = 2.5 will define the maximum of $Q^{-1}(\omega) \approx 0.17$, which is close to the observed value of the internal friction maximum.

Discussion

The anelastic high-temperature dynamic response of the MACOR sample has been observed at temperatures below and above $T_g \sim 600$ °C of the alumino-borosilicate matrix which may be roughly estimated from the thermal expansion coefficient measurements. There are a number of relaxation mechanisms that may be involved in the anelastic behaviour of the MACOR glass-ceramic aggregate.

1. A rigid suspended particle may rotate under shear stress. The angle of rotation of solid spherical particles in viscous liquid has a characteristic relaxation time

$$\tau_{\text{rot}} \propto \tau_{Max}\ \frac{G_\infty^{liquid} d^3}{kT} \tag{3}$$

where τ_{Max} is the Maxwell relaxation time of a liquid phase, d is the size of a suspended particle, G_∞^{liquid} is the unrelaxed shear modulus of the liquid, and kT is the thermal energy scaling factor (Landau and Lifshitz 1987). For suspensions of particles with a wide distribution of sizes this relaxation mechanism may be effectively hidden by the viscoelasticity of the liquid itself (τ_{Max}) due to the strong dependence on the particle size $\propto d^3$. For the large size particles the contribution of this relaxation mechanism may be significant and results in the weak deviation from the Maxwell liquid behaviour at low frequencies even in dilute suspensions.

2. At low concentrations of melt ($\varphi < 0.1$) when the width between particles becomes much less than the size

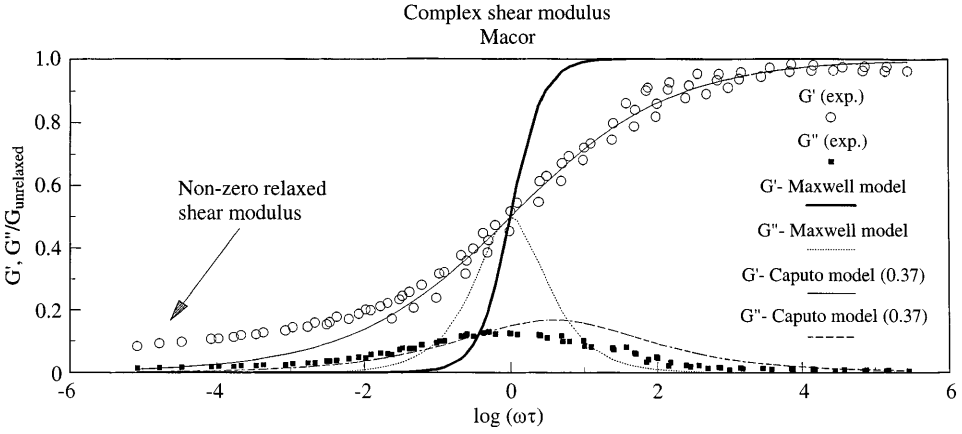

Fig. 5 Normalised real and imaginary components of the complex shear modulus of MACOR sample as a function of the normalised frequency ωτ in comparison with a Maxwell model and a Caputo model

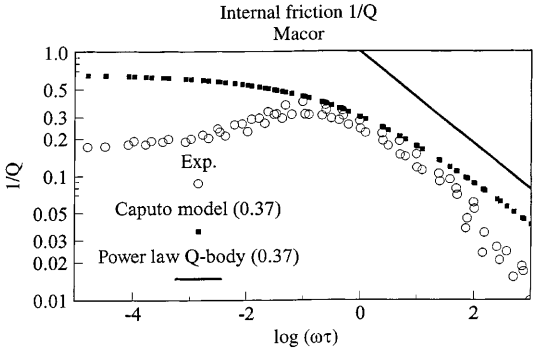

Fig. 6 Internal friction Q^{-1} of MACOR sample as a function of the normalised frequency ωτ compared with a Caputo model and a power law Q-body with the exponent = 0.37

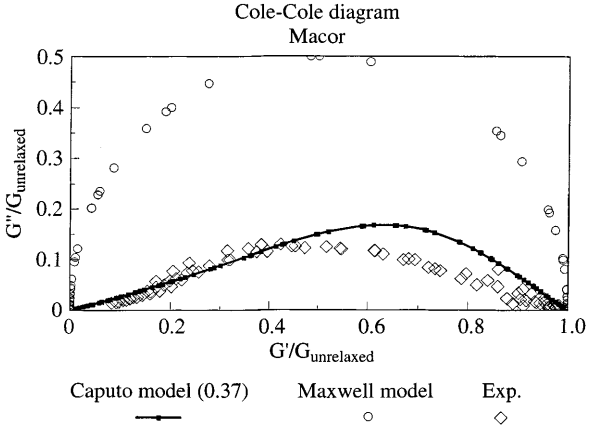

Fig. 7 Cole-Cole diagram of MACOR sample in comparison with Maxwell and Caputo models

of particles, the dominant mechanism in the anelastic behaviour in solid–liquid aggregate is probably an intergrain sliding in the presence of highly liquid phase. Even when grain boundaries are wetted with viscous melt or glassy phase, the strain rate on a solid–liquid interface will be limited either by a diffusion of components dissolving in the melt, or by the rate of solid phase dissolution in the melt (Gueguzin 1967). *By analogy* with the grain boundary sliding in polycrystalline solids (e.g. Kê 1949; Nowick and Berry 1972) the relaxation time of this process is as follows

$$\tau_{\text{g.b.}} \propto \frac{\mu}{G_{\infty}^{solid}} \frac{d}{b} \tag{4}$$

where μ is the shear viscosity of liquid phase, G_{∞}^{solid} is the unrelaxed shear modulus of solid phase matrix, and b is the thickness of the grain boundary or the melt layer with the effective shear viscosity η.

Under a shear deformation the sliding between crystal grains will proceed and stresses will grow at the places where grain boundaries have contacts (Raj and Ashby 1971). Sliding of grain boundaries stops when elastic response of grains compensate the applied shear stress. The recovery, upon the removal of the applied shear stress, is time-delayed with a characteristic relaxation time. The shear stress response, thus, is scaled by the shear viscosity of the melt phase (or the viscosity of the intergranular liquid) and the unrelaxed modulus of solid phase. The modification of the expression for the grain boundary sliding relaxation accounting for non-planar grain boundaries results in a modification of Eq. (4) to $\tau_{g.b.} \propto \frac{1.14(1-\nu^2)\mu}{E}\frac{d}{b}$, where ν is Poisson's ratio and E is Young's modulus of solid phase (Mosher and Raj 1974). The activation energy of this relaxation time is equal to the activation energy of the grain boundary viscosity or diffusion in the case of a very small fraction of melt phase. At large strains the melt phase in this case acts as a rapid diffusion path providing a redeposition of the crystalline phase from regions under compression into regions under tension (Raj 1982).

Besides the pressure solution or diffusional type model of the liquid-enhanced creep there is a lubricant flow model (Dryden et al. 1989), in which the liquid phase facilitates the sliding of grains over each other more easily. The relaxation time of a liquid flow between grains estimated via the effective shear viscosity of the aggregate should be proportional to (d/b) for the square grain array or plane boundaries (Pharr and Ashby 1983) and to $(d/b)^3$ for the hexagonal grain array (Dryden et al. 1989).

The additional relaxation of the 'melt squirt' (Mavko and Nur 1975) in crystal-melt aggregates may occur as melt flows from one grain boundary or triple junction to another. The calculated relaxation time for the flow between triangular tubes is proportional to $(d/b)^2$ (Mavko 1980) and for flow between plane films it is $\propto (d/b)^3$ (O'Connel and Budiansky 1977).

3. At intermediate volume fractions of melt ($\varphi \approx 0.55$–0.45) crystals start to form a weak structure or framework, i.e. the shear modulus of the crystal 'skeleton' may be small but non-zero. This fact is supported by theoretical modelling of the elastic moduli of composite materials with rigid disc-shape inclusions (e.g. Wu 1966). The mechanical response of disc-shape inclusions is similar to plane cuts, so that their effect on the 'strengthening' of the overall bulk and shear moduli is higher than that from spherical inclusions, providing (the bulk and shear modulus of the inclusions is much stronger than those of the matrix (Walpole 1969). For a soft matrix containing elongated (fabric- or planar-shape) rigid inclusions the physical principle of composite 'strengthening' can be formulated as: the interconnected rigid phase carries greater stress, while the soft viscous phase tends to take greater strain with reference to the volume fraction ratio (e.g. Ji and Zhao 1994). Thus, if the unrelaxed shear modulus of the crystal skeleton is not zero, *by analogy* with the previous case the relaxation time of the intergrain slip (i.s.) can be written as follows.

$$\tau_{\text{i.s.}} \propto \tau_{Max} \frac{G_{\infty}^{liquid}}{G_{\infty}^{solid}} \frac{d}{b} \propto \tau_{Max} F(\sqrt[3]{\varphi}). \tag{5}$$

In Eq. (5) F(φ) is an empirical function depending on the volume fraction of liquid phase φ. When φ is known the d/b ratio can be estimated for a suspension consisting of the centred cubic array of spherical particles (Ungarish 1993) or for an array of hexagonal grains (Dryden et al. 1989). The ratio of shear moduli in Eq. (5) may be calculated by using the self-consistent estimate (Walpole 1969; Hill 1965).

If crystals in the solid-liquid suspension have disc-shapes with large aspect ratio d/h, where h is the thickness of discs, then another two mechanisms may contribute to the anealstic behaviour of crystal-melt aggregates. These may be flexural and torsional deformation modes of crystals surrounded by a viscous liquid. In both cases the characteristic relaxation time is a power law function of the aspect ratio of a crystal shape and may be expressed as follows (see Appendix):

$$\tau_{\sigma(Torsional)} \propto \left(\frac{d}{h}\right)^4 \cdot F(\sqrt[3]{\varphi}) \cdot \left(\frac{G_{\infty}^{Liquid}}{G_{\infty}^{Solid}}\right) \cdot \tau_{Max}, \tag{6}$$

and

$$\tau_{\sigma(Flexural)} \propto \left(\frac{d}{h}\right)^6 \cdot F(\varphi) \cdot \left(\frac{G_{\infty}^{Liquid}}{G_{\infty}^{Solid}}\right) \cdot \tau_{Max.} \tag{7}$$

In both cases the characteristic relaxation time is a strong function of the aspect ratio d/h with the exponent 4–6 and appears to be a much weaker function of the volume fraction of crystals φ. When $d/h \gg 1$ this mechanism of relaxation may be slower than the viscoelastic relaxation of the surrounding matrix and can be observed at low frequencies and temperatures, i.e. above the glass transition temperature of the vitreous matrix.

As the volume concentration of suspended particles increases (d/b increases), grains are closer and the relaxation due to the grain interaction ($\tau_{i.s.}$) increases. Thus, at a certain critical concentration of melt φ_{cr}. the rotation + torsion + bending modes of crystal relaxation may be appreciable in the relaxation spectrum and can be resolved experimentally by measuring the complex shear modulus and internal friction at low frequencies and temperatures. In this case the complex shear modulus will have a non-zero plateau at $\omega\tau \to 0$. The wide distribution in the width of grain contacts which can be assumed in the MACOR glass ceramic may result in a flattening out of the internal friction peak in Figs. 3 and 5. This relaxation peak may be unobservable in crystal-melt suspensions with a smaller aspect ratio of crystals.

The effect of the aspect ratio of mica crystals on the microhardness increase has been observed experimentally for MACOR samples (Baik et al. 1997). The same volume fraction of crystals with an aspect ratio 10 provides a much higher microhardness because of much better connectivity (effective crystallinity) of disc-shape crystals in comparison with isotropic (spherical) ones (Baik et al. 1997). These authors use a conception of the effective crystallinity, a crystal fraction which equals to a hypothetical volume fraction of spherical shape crystals when a suspension possesses the same percolation properties as a suspension with elongated crystals. The effective crystallinity may be calculated from the volume fraction of crystals $(1 - \varphi)$ and the aspect ratio (d/h) as follows:

$$\varphi_{eff} = 1 - (1 - \varphi)^{\left[\frac{(d/h)^{2/3} + 2(d/h)^{-1/3}}{3}\right]^{3/2}} \tag{8}$$

(Baik et al. 1997). From Eq. (8) the effective crystallinity of 55 vol% of disc-shape crystals with an aspect ratio 10 is about 87 vol%.

The mechanisms other than these already listed are unlikely to contribute substantially to the observed anelastic behaviour of the MACOR glass-ceramics. However the following should be noted:

A. The anisotropic elastic properties of mica crystals, which may result in the anelastic behaviour of aggregate at low temperatures–high frequency range of $\omega\tau$ (below the softening temperature). In this case the internal friction peak is due to the motion of basal-plane dislocations in mica grains under flexure and may be effectively resolved only below the glass transition of the matrix. The activation energy of this peak would correspond to the dislocation creep in [001] plane because it is the weakest one. In a natural single biotite crystal, having OH : F = 2 : 3, the activation energy of the disclocation creep in this direction is *Ea*

$\sim$ 82 kJ/mol (Kronenberg et al. 1990). Although the fluorinated phlogopite does require higher electrostatic energy to separate mica layers than OH-phlogopite, 110–120 and 88–94 kJ/mol for F- and OH-phlogopite, respectively (Giese 1984), we may not expect that the activation energy of the dislocation creep in pure F-phlogopite is three times higher than in a natural biotite sample.

B. In a wide range temperatures the alumino-borosilicate glass matrix may possess a non-Arrhenian viscosity due to the effect of boron. The non-Arrhenian rheology can complicate the rheological behaviour of the MACOR sample at high temperatures (the data dispersion on master curves may be attributed to this effect) but will not result in the anelastic properties (non-zero shear modulus). The observed Arrhenian dependence of the internal friction peak maximum is valid only for the temperature range of experiments.

C. At high temperatures borosilicate melt may have non-Newtonian viscosity due to the nm-scale phase separation. In this case small inclusions of a low viscosity melt (enriched in B_2O_3) will decrease the relaxation modulus and therefore lead to a decrease of the melt stiffness (Habeck et al. 1990), the MACOR samples has an increase of the relaxed shear modulus. The effect of the non-Newtonian rheology of the phase-separated emulsion will be important for experiments in a wide range of stresses, which was not the case in this study.

Thus, the presence of elongated crystal particles in the viscoelastic silicate melt results in at least three additional mechanical relaxation processes in comparison with viscoelastic liquid: rotation, flexure deformation and sliding of crystals. The grain rotation and sliding as mechanisms of the internal friction are significant in concentrated suspensions, especially with elongated and plane-shape particles, and correspond to the first rheological threshold, i.e. non-zero shear modulus of mixture (e.g. Bagdassarov et al. 1994). In dilute suspensions of crystals + silicate melts this mechanism is unobservable due to the shear stress relaxation in the liquid itself and a zero shear modulus of a dilute suspension. At a given concentration of solid phase suspended in the liquid, the grain bending and rotation are more effective for an aggregate with elongated and plane-shape solid particles with a higher aspect ratio ($d/h \gg 1$) and large number of mechanical contacts (tabular- or disc-shaped crystals).

The dependence of $\log[Q^{-1}(\omega\tau)]$ at high temperatures and low strain-rates decreases linearly with $\omega\tau$ increase. By contrast, at high concentrations of crystals (>85 vol%) the behaviour of aggregates may be effectively described as a standard anelastic solid (Green et al. 1990). The viscoelastic Burgers body describes well the overall deformation response obtained on olivine + 12 vol% basalt melt aggregates and β-spodumene + 2 vol% LAS glass-ceramic (Cooper et al. 1989), enstatite + 5 vol% glass-ceramic (Cooper 1990). At higher strains when the transient creep is accomplished, the viscoelastic behaviour can be approximated by a Maxwell body under shear deformation, whereas under the pure compressive deformation the observed anelastic response associates with a standard anelastic solid (Green and Cooper 1993). The activation energy of the main time in the spectrum is equal to the activation energy of dislocation or defect diffusion. Relaxation of shear stresses is due to the amorphous behaviour of grain boundaries. These mechanisms of the internal friction results in a resolved peak on the plot $\log[Q^{-1}(\omega\tau)]$, where the amplitude of the peak is proportional to the grain size, and the characteristic time of the peak is a function of grain aspect ratio and the volume fraction of melt in the suspension. When the volume fraction of crystals decreases from 85 to 40 vol%, the amplitude of the peak decreases and it shape degenerates to a plateau. The viscoelastic behaviour in this case may be fit to a Caputo model with the parameter $\approx$0.45 (Bagdassarov et al. 1994). The physical sense of the rheological threshold at 40 vol% of crystals is that at higher concentrations of solid particles the internal friction and mechanical dissipation increases at high strain-rates and then decreases at low strain rates. At this critical concentration it is impossible to add more solid particles in the mixture without changing the average co-ordination number or without increasing the short range positional ordering in the suspension (Pusey and van Megen 1986). Progressively more solid particles are in contact and their relative motion is significantly reduced (Esquivel-Sirvent et al. 1995). This behaviour is a starting point for "rigidity" of a suspension or non-zero shear modulus at low strains (a threshold rigid particle concentration in the yield stress conception for concentrated suspensions) (e.g. Ryerson et al. 1988). If all particles were of a uniform size, spherical shape and ideally rigid, the second rheological threshold will be at 63.7 vol% of crystal concentration. In reality, solid grains themselves possess creep properties due to dislocation and defect diffusion, amorphous grain boundary structure etc. which is why the second rheological threshold is not well defined in partially molten rocks, where crystal shape and crystal boundaries are rather irregular.

Conclusions

1. In samples of MACOR glass-ceramics, representing a crystal-melt aggregate of 55 vol% of sheet-like particles, a resolved high-temperature peak of the internal friction is observed at temperature above the glass transition temperature of the glass matrix. This may indicate a significant mechanical grain interaction in this type of material.
2. MACOR glass-ceramics possesses a non-zero-shear modulus at temperatures above the glass transition temperature of the glass matrix.
3. By comparing the viscoelastic behaviour of the suspension of spherical and sheet-like crystals it may be concluded that the amplitude of the internal friction

peak associated with crystal rotation and deformation increases with a increase of the aspect ratio of crystals suspended in the melt.

Acknowledgements The author thanks Dr. S. Webb (ANU) for the sample of MACOR glass-ceramic and the help with ultrasonic measurements.

Appendix

This is concerned with an anelastic behaviour and mechanical relaxation associated with flexural and bending deformation modes of crystals suspended in a viscous matrix with viscosity μ. We consider for simplicity a crystal-glass aggregate as a regular array of disc-shape crystals with the size $d \times d$ and thickness h, d/h is the aspect ratio. Here we assume that $d \gg h$. The average distance between crystals is b ($b < d$). According to the formal theory of relaxation (Nowick and Berry 1972) the decay of flexural stress (bending of crystals) or the decay of an angular momentum (torsion of crystals), and the respective growth of flexural strain or twist deformation $\Delta\xi$, will be a simple exponential function. Under constant applied stress to the sample, the corresponding relaxation equation for the amplitude of a flexural deformation or of a torsion deformation $\Delta\xi$ of an individual crystal is

$$\Delta\xi = \frac{\left(\Delta\xi - \Delta\bar{\xi}\right)}{\tau_\sigma} \tag{A1}$$

where $\Delta\bar{\xi}$ is the final equilibrium strain for constant stress and τ_σ is the relaxation time (e.g. Nowick and Berry 1972). We may specify that at $t = 0$, $\Delta\xi = 0$, and the relaxation time may be estimated from a final equilibrium strain and an initial strain velocity:

$$\tau_\sigma = \frac{\text{A(amplitude of bending deformation)}}{\text{V}_0\text{(initial linear velocity)}}$$

for flexure mode, (A2)

$$\tau_\sigma = \frac{\alpha\text{(angle amplitude of torsion deformation)}}{\Omega_0\text{(initial angular velocity)}}$$

for torsion mode of crystal deformation. (A3)

The maximum amplitude of the flexural deformation of a plate $d \times d$ having a Young modulus E, Poisson ratio v, thickness h, under the force F applied at its centre at free boundary conditions is:

$$A = \frac{12(1-v)F}{16\pi E h^3} d^2 (3+v), \tag{A4}$$

(Landau and Lifshitz 1987b).

A maximum of the viscous drag force acting between two parallel plates of a size $d \times d$, moving to each other with a velocity V_o and squirting a liquid with a shear viscosity μ is:

$$F = \frac{3\pi\mu V_o d^4}{32 b^3} \tag{A5}$$

where b is the distance between plates (Landau and Lifshitz 1987a). After substitution of F in Eq. (A4) and combining Eqs. (A5) with (A2), we obtain

$$\tau_{\sigma(Flexural)} = \frac{9}{128} \cdot \frac{(1-v)(3+v)}{2(1+v)} \cdot \left(\frac{d}{h}\right)^6 \cdot \left(\frac{h}{b}\right)^3 \cdot \frac{\mu}{G}, \tag{A6}$$

where G is the unrelaxed shear modulus of disc-shape crystals.

The angle deformation of a plate $d \times d$ with a shear modulus G and a thickness h under the torsion momentum M_t applied in the direction of d is:

$$\alpha = \frac{3M_t}{Gh^3}. \tag{A7}$$

From other side the maximum torque of the viscous force acting on a plate $d \times d$ rotating with the angular velocity Ω_o in the direction d in a liquid with a shear viscosity μ is:

$$M_t = \frac{\pi d^3}{3}\mu\Omega_o$$

or

$$M_t = \frac{\pi d^3}{3}\frac{d}{b}\mu\Omega_o, \tag{A8}$$

if the average distance between plates $b \ll d$. From Eqs. (A3, A7–8) , we obtain

$$\tau_{\sigma(Torsional)} = \pi\left(\frac{d}{h}\right)^4 \cdot \frac{h}{b} \cdot \frac{\mu}{G}. \tag{A9}$$

References

Bagdassarov NS, Dingwell DB (1993) Frequency dependent rheology of vesicular rhyolite. J Geophys Res 98: 6477–6487

Bagdassarov NS, Dorfman AM (1998) Viscoelastic behavior of partially molten granites. Tectonophysics, 290 (1/2): 27–45

Bagdassarov NS, Dingwell DB, Webb SL (1994) Viscoelasticity of crystal- and bubble-bearing rhyolite melts. Phys Earth Planet Inter 83: 83–89

Baik DS, No KS, Chun JS, Yoon YJ, Cho HY (1995) A comparative method of machinability for mica based glass-ceramics. J Mater Scie 30: 1801–1806

Baik DS, No KS, Chun JS, Cho HY (1997) Effect of the aspect ration of mica crystals and crystallinity on the microhardness and machinability of mica glass-ceramics. J Mater Process Technol 67: 50–54

Beall GH (1972) Mica glass-ceramics, United States Patent 3,689,293.

Beall GH, Chyung C-K, Watkins HJ (1974) Mica glass-ceramics. United States Patent 3,801,295.

Beall GH, Chyung K, Hoda SN (1978) Glass-ceramics displaying inherent lubricity. United States Patent 4,118,237

Berckhemer H, Kamfmann W, Aulbach E (1982) Anelasticity and elasticity of mantle rocks near partial melting. In: Schreyer W (ed) High-pressure researches in geoscience. E. Schwaizerbart'sche Verlagsbuchhandlung, Stuttgart, pp 113–132

Caputo M (1967) Linear models of dissipation whose Q is almost frequency independent - II. Geophys J R Astron Soc 13: 529–539

Cooper RF, Kohlstedt DL, Chyung K (1989) Solution precipitation enhanced creep in solid-liquid aggregates which display a non zero dihedral angle. Acta Metall 37: 1759–1771

Cooper RF (1990) Differential stress-induced melt migration: an experimental approach. J Geophys Res 95: 6979–6992
Day DE, Rindone GE (1961) Internal friction of progressively crystallised glasses. J Am Cer Soc 44: 161–167
Dingwell DB, Knoche R, Webb SL, Pichavant M (1992) The effect of B_2O_3 on the viscosity of haplogranitic liquids. Am Mineral 77: 457–461
Dryden JR, Kucerovsky D, Wilkinson DS, Watt DF (1989) Creep deformation due to a viscous grain boundary phase. Acta Metall 37: 2007–2015
Esquivel-Sirvent R, Green DH, Yun SS (1995) Critical behavior in the fluid/solid transition of suspensions. Appl Phys Lett 67: 3087–3089
Gueguzin YF (1967) Physics of sintering. Nauka Publishing House, Moscow, 360 pp (in Russian)
Giese RF Jr (1984) Electrostatic energy models of micas. In : Micas. (ed Bailey SW) Reviews in Mineralogy 13: Mineralogical Society of America, Washington: 129
Green DH, Cooper RF (1993) Dilatational anelasticity in partial melts: viscosity, attenuation, and velocity dispersion. J Geophys Res 98: 19,807–19,817
Green DH, Cooper RF, Zhang S (1990) Attenuation spectra of olivine/basalt partial melts: transformation of Newtonian creep response. Geophys Res Lett 17: 2097–2100
Habeck A, Hessenkemper H, Brückner R (1990) Influence of microheterogeneities on the mechanical properties of high-viscous melts. Glastech Ber 63: 111–117
Hill R (1965) A self-consistent mechanics of composite materials. J Mech Phys Solids 13: 213–222
Jackson I, Niesler H, Weidner D (1981) Explicit correction of ultrasonically determined elastic wave velocities for transducer – bond phase shift. J Geophys Res 86: 3736–3748
Ji S, Zhao P (1994) Strength of two-phase rocks: a model based on fibre-loading theory. J Struct Geology 16: 253–262
Kê T-S (1949) A grain boundary model and the mechanism of viscous intercrystalline slip. J Appl Phys 20: 274–280
Kronenberg AK, Kirby SH, Pinkston J (1990) Basal slip and mechanical anisotropy of biotite. J Geophys Res 95: 19, 257–19,278
Landau LD, Lifshitz EM (1987a) Fluid mechanics. Course of theoretical physics, vol 6, 2 edn, Pergamon Press, New York, 730 pp
Landau LD, Lifshitz EM (1987b) Theory of elasticity. Course of theoretical physics, vol 7, 2 edn, Pergamon Press, New York, 249 pp
Lawn BR, Padture NP, Cai H, Guiberteau F (1994) Making ceramics "ductile". Science 263: 1114–1116
Mavko GM (1980) Velocity and attenuation in partially molten rocks. J Geophys Res : 85: 5173–5189
Mavko GM, Nur A (1975) Melt squirt in the asthenosphere. J Geophys Res 80: 1444–1448
Mosher DR, Raj R (1974) Use of the Internal friction technique to measure rates of grain boundary sliding. Acta Metall 22: 1469–1474
Nowick AS, Berry (1972) Anelastic relaxation in crystalline solids. Academic Press, New York, 677 pp
O'Connel RJ, Budiansky B (1977) Viscoelastic properties of fluid-saturated cracked solids. J Geophys Res 82: 5719–5735
Pharr GM, Ashby MF (1983) On creep enhanced by a liquid phase. Acta Metall 31: 129–138
Pusey PN, Megen W van (1986) Phase behavior of concentrated suspensions of nearly hard colloidal spheres. Nature 320 : 340–342
Raj R (1982) Creep in polycrystalline aggregates by matter transport through a liquid phase. J Geophys Res 87: 4731–4739
Raj R, Ashby MF (1971) On grain boundary sliding and diffusional creep. Metal Trans 2: 1113–1127
Raj R, Chyung CK (1981) Solution-precipitation creep in glass ceramics. Acta Metall 29: 159–166.
Ryerson FJ, Weed HC, Piwinskii AJ (1988) Rheology of subliquidus magmas. 1. Picritic compositions. J Volcanol Geotherm Res 93: 3421–3436
Tsai RL, Raj R (1980) The role of grain-boundary sliding in fracture of hot-pressed Si_3N_4 at high temperatures. J Am Ceram Soc 63: 513–517
Versteeg VA, Kohlstedt DL (1994) Internal friction in lithium aluminosilicate glass-ceramics. J Am Ceram Soc 77: 1169–1177
Ungarish M (1993) Hydrodynamics of suspensions. Springer-Verlag, Berlin Heidelberg New York
Walpole LJ (1969) On the overall elastic moduli of composite materials. J Mech Phys Solids 17: 235–251
Weimer AT, MaNghNaNi MH, Rishi R (1987) Internal friction in tholeiitic Basalts. J Geophys Res 92: 11035–11043
Wu TT (1966) The effect of the inclusion shape on the elastic moduli of a two-phase material. Int J Solid Struct 2: 1–8